Method for Image Quality Evaluation of Satellite-based SAR Data

Kohei Arai[1], Michihiro Mikamo[2], Shunsuke Onishi[3]
Faculty of Science and Engineering, Saga University, Saga, Japan[1]
Institute for Q-shu Pioneers of Space, Inc. (iQPS), Fukuoka, Japan[2, 3]

***Abstract*—A method for image quality evaluation of satellite-based Synthetic Aperture Radar: SAR data is proposed. Not only geometric fidelity but also signal to noise ratio, frequency component, saturated pixel ratio, speckle noise, optimum filter kernel size and its filter function are evaluated. Through experiments with SAR so called QPS-SAR_2 (Q-shu Pioneers of Space SAR the second) of imagery data, all these items are evaluated, and it is confirmed that the geometric and radiometric performances are good enough. Also, geometric fidelity of QPS-SAR_2 is compared to Sentinel-1/SAR European Space Agency (ESA) provided data which is obtained on the same day of QPS-SAR_2 data acquisition.**

Keywords*—Image quality; synthetic aperture radar (SAR); geometric fidelity; signal to noise ratio; frequency component; saturated pixel ratio; speckle noise; optimum filter kernel size; filter function for speckle noise reduction

I. Introduction

Institute for Q-shu Pioneers of Space, Inc.: iQPS has realized a mass of 1/20 and a cost of 1/100 of the conventional X band SAR satellite by using a lightweight antenna for small satellites developed in-house, and a 100 kg class high-definition small SAR. It was the first successful SAR mounted small satellite in Japan. Currently, we are aiming to launch 36 small SAR satellites and build a constellation early after 2025, and to provide a quasi-real-time ground observation data service about every 10 minutes. To realize this project, we were able to work on the development, manufacture, and launch of two satellites, "Izanagi" and "Izanami" which play the role of technology demonstrator. The first unit "Izanagi" was launched in December 2019, and the second unit "Izanami" was launched after February 2021.

The satellite called "Izanami" which was developed and manufactured by iQPS and about 20 local companies in Kyushu was launched by the flagship rocket "Falcon 9" of the American space development company "SpaceX" on January 25, 2021 (Monday). It was launched at 1:14 a.m. and set to the altitude of about 525 km. Then, on the same day, the first communication was successful, the retractable antenna was deployed on the 30th of January (Saturday), and the first image acquisition was announced on 3 March (Wednesday), about one month after the launch. After that, Izanami continued to observe steadily every day, and succeeded in acquiring an image with an azimuth resolution of 70 cm and a range (ground range) resolution of 70 cm in a high-definition mode (spotlight mode)[1] with a resolution of 70 cm.

The need for high-definition images in the market is extremely high, and the successful acquisition and demonstration of technology at Unit 2 Izanami (QPS-SAR_2) is a major step toward the full-scale data provision service business. In the future, we will further stabilize the image quality and proceed with the development of the usage platform with a sense of speed.

There are many papers which deal with SAR image quality evaluation methods. Not only geometric fidelity but also signal to noise ratio, frequency component, saturated pixel ratio, speckle noise, optimum filter kernel size and its filter function can be evaluated with the previously proposed methods. Cross comparison between two different SARs which are onboarded the different satellites and observe in a same day is conducted. This is a new method for the SAR imagery data quality evaluation in this paper. Two different SARs observed the same ground cover target with the different off-nadir angles. Therefore, layover, shadowing, foreshortening is different each other of SAR imagery data results in some processing is required for tie point matching. Otherwise, pixel-to-pixel comparisons cannot be performed. The purpose of this paper is to propose SAR image quality evaluation methods such as spatial resolution, signal to noise ratio, modulation transfer function, pixel geolocation accuracy (geometric fidelity), etc. Through the experiments, it is found that the proposed method works well for image quality evaluation.

In the next section, related research works are described followed by research background and theoretical background. Then, the proposed system is described at first followed by some experiments are described together with conclusion and some discussions.

II. Related Research Works

The following are the SAR related papers,

A method for Ground Control Point: GCP acquisition using simulated SAR derived from Digital Elevation Model: DEM is proposed [1] together with GCP acquisition using simulated SAR imagery data and evaluation of GCP matching accuracy with texture features [2].

[1]There are normal mode (stripmap mode) with a resolution of 1.8m (azimuth resolution 1.8m x range resolution 0.7m) and high-definition mode (spotlight mode) with a resolution of 70cm.

Speckle noise removal of SAR images with DEM is attempted [3]. Meantime, a method of speckle noise reduction for SAR data is proposed [4]. Meanwhile, SAR image classification based on Maximum Likelihood decision rule: MLH with texture features taking into account a fitness to the probability density function is proposed [5]. A new method for SAR speckle noise reduction (Chi-Square Filter: CSF) is proposed and validated [6] together with a new method for SAR speckle noise reduction based on CST filter [7].

Decomposition of SAR polarization signatures by means of eigen-space representation is attempted [8]. On the other hand, evaluation of vector winds observed by NASA Scatterometer: NSCAT in the ocean of Japanese vicinity is conducted [9].

Polarimetric SAR image classification with maximum curvature of the trajectory in eigen space domain on the polarization signature is proposed [10] together with polarimetric SAR image classification with maximum curvature of the trajectory in eigen space domain on the polarization signature [11]. Meanwhile, polarimetric SAR image classification with high frequency component derived from wavelet Multi Resolution Analysis: MRA is proposed [12].

Comparative study of polarimetric SAR classification methods including proposed method with maximum curvature of trajectory of backscattering cross section in ellipticity and orientation angle space is conducted [13]. On the other hand, wavelet MRA and its application to polarimetric SAR classification are proposed [14].

Sentinel-1A SAR data analysis for disaster mitigation in Kyushu, Japan is conducted [15]. Also, flood damage area detection method by means of coherency derived from interferometric SAR analysis with Sentinel-1A SAR is proposed [16]. GCP generation from simulated SAR image derived from Digital Terrain Model: DTM and its application to texture feature extraction is conducted [17].

Meanwhile, there are the following not only SAR but also optical sensor image quality evaluation related papers,

Report on vicarious calibration and image quality evaluation of LISA/LISAT[2] is presented and issued [18]. Also, methods for vicarious calibration and image quality evaluation of LISA/LISAT are proposed [19].

On the other hand, there are the following papers which deal with frequency component analysis,

Polarimetric SAR image classification with high frequency component derived from wavelet multi resolution analysis: MRA is proposed [20]. Meanwhile, hearing aid method by equalizing frequency response of phoneme extracted from human voice is proposed [21].

Meanwhile, the following papers deal with noise analysis,

On the other hand, sensitivity analysis of Fourier Transformation Spectrometer: FTS against observation noise on retrievals of carbon dioxide and methane is conducted [22].

Noise suppressing edge enhancement based on Genetic Algorithm: GA taking into account complexity of target image measured with Fractal dimension is proposed [23]. Meantime, a method for aerosol parameter estimation error analysis is proposed with a consideration of noises included in the measured solar direct and diffuse irradiance [24].

Method of noise reduction in passive remote sensing is proposed for noise and clutter rejection [25]. On the other hand, speckle noise removal of SAR images with DEM is proposed [26]. Flood damage area detection method by means of coherency derived from interferometric SAR analysis with Sentinel-1A SAR is proposed [27]. Furthermore, Ground Control Point: GCP generation from simulated SAR image derived from Digital Terrain Model: DTM and its application to texture feature extraction is also proposed and validated [28]. Meanwhile, method for frequent high resolution of optical sensor image acquisition using satellite-based SAR image for disaster mitigation is proposed [29].

III. Theoretical Background and Proposed Method

Not only geometric fidelity but also Signal to Noise ratio: S/N, frequency component, saturated pixel ratio, speckle noise, optimum filter kernel size and its filter function can be evaluated with the previously proposed methods.

As for the geometric fidelity, GCPs which are derived from geographic maps can be used. S/N can be evaluated with the ratio of mean and standard deviation of certain homogeneous areas. Frequency component can be evaluated with Fast Fourier Transformation: FFT, Discrete Cosine Transformation: DCT and so on.

On the other hand, saturated pixel ratio can be evaluated with histogram analysis. As for the speckle noise evaluation, visual perception can be used for identification of saturated pixels. Meanwhile, optimum filter kernel size and its filter function for speckle noise reduction can be estimated with trial and errors through visual perception.

Cross comparison between two different SARs which have onboarded the different satellites and observed in a same day is conducted. This is a new method for the SAR imagery data quality evaluation in this paper. Two different SARs observed the same ground cover target with the different off-nadir angles. Therefore, layover, shadowing, and foreshortening are different from each other in SAR imagery data, resulting in the need for some processing to be done for tie point matching. Otherwise, pixel-to-pixel comparisons cannot be performed.

IV. Experiments

A. Examples of Acquired QPS-SAR_2 Imagery Data used for Image Quality Evaluation

Fig. 1 shows examples of acquired QPS-SAR_2 imagery data used for image quality evaluation. Fig. 1(a) and 1(b) are SAR images of Osaka, Japan (34.69N, 135.50E) (these are referred to Osaka scenes hereafter) which are acquired at 9:24 p.m. (Japan time) on 4 May 2021 (Tuesday) while Figure 1(c) to (g) are SAR images of Tokyo, Japan (N35 40', E139 46') (these are referred to Tokyo scenes hereafter) which are acquired at 9:06 p.m. (Japan time) on 23 March 2021 (Friday).

[2]https://www.eoportal.org/satellite-missions/lapan-a3#overview

In Fig. 1(a), "Senri Chuo Station" (Located in 1-chome Shinsenri Higashimachi (34.81N, 135.49E), Toyonaka City, Osaka Prefecture, it is a station on the Kita-Osaka Kyuko Railway Namboku Line and the Osaka Monorail Main Line.) is a little to the right of the central part. In Fig. 1(b), the steel tower and a part of the electric wire in the upper left, the Ferris wheel "OSAKA WHEEL" and "Panasonic Stadium Suita" with a height of 123m in the lower left, and the monorail stopped in the garage near the center are identified. The detail locations of Toyonaka and Osaka wheel are shown in Fig. 1(c).

As for Fig. 1(f), since the roof of the Tokyo Dome (35.71N, 139.75E) can be seen through, you can even see the electric bulletin board. Meanwhile, in Fig. 1(g), you can see Ueno Onshi Park (35.72N,139.77E) and Shinobazu Pond (35.71N, 139.77E) while you can identify the freight container in the lower right in Fig. 1(h). The detail locations of Tokyo Marunouchi buildings (35.68N, 139.76E), Minami Senju (35.73N 139.80E), Tokyo dome and Ueno Onshi Park are shown in Fig. 1(i).

Through comparisons between geographic maps and QPS-SAR_2 imagery data, it is found that the spatial resolution (equivalent to ground range) of QPS-SAR_2 is confirmed as 70cm (Azimuth resolution 70cm while range resolution 70cm).

(a) Toyonaka City, Osaka Prefecture

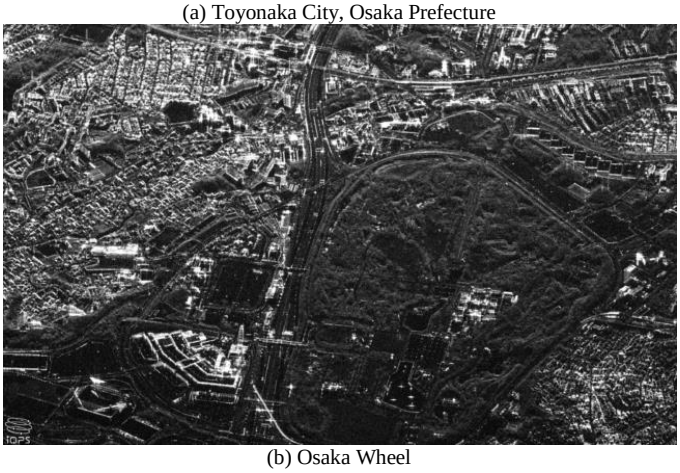

(b) Osaka Wheel

(c) Locations of Toyonaka and Osaka wheel

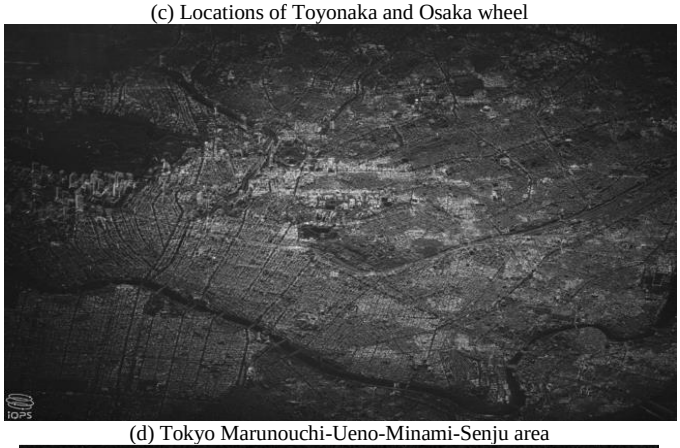

(d) Tokyo Marunouchi-Ueno-Minami-Senju area

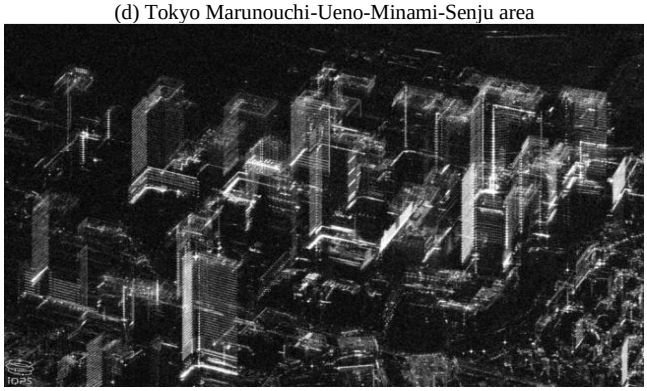

(e) Marunouchi Buildings

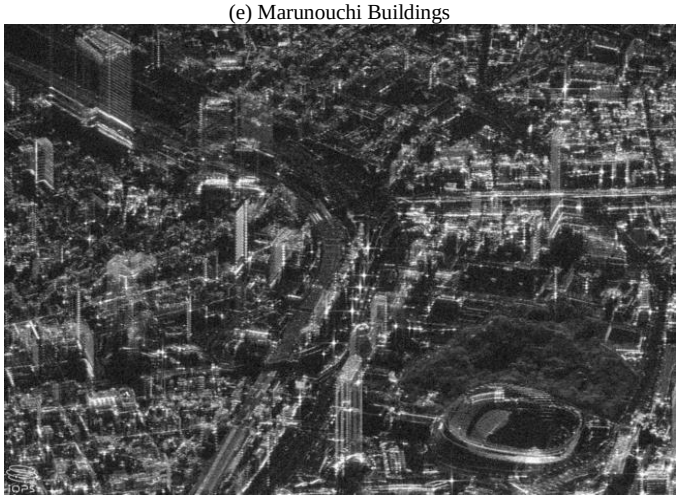

(f) Around Tokyo Dome City

(g) Around Ueno Onshi Park

(h) Around Minami-Senju Station

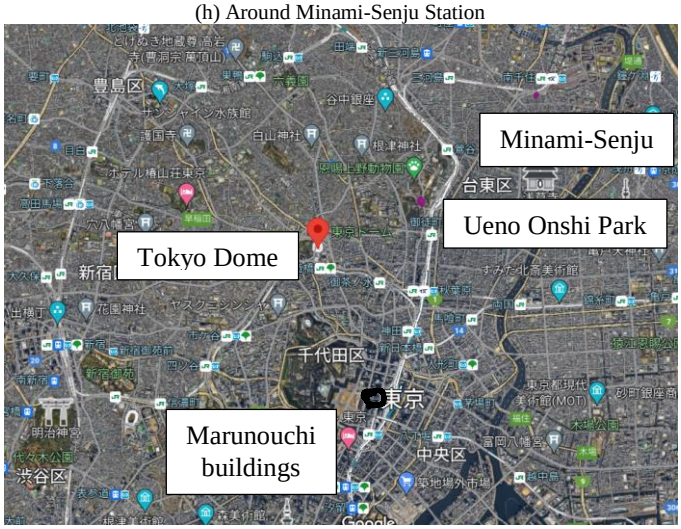

(i) Locations of Minami-Senju, Ueno Onshi park, Tokyo dome, Marunouchi buildings and Tokyo station

Fig. 1. Examples of the acquired QPS-SAR_2 imagery data.

From the QPS-SAR_2 image, edge responses are reduced. Then, differentiations of the responses are calculated. After that, frequency component analysis is made for the differentiations result in spatial resolution.

B. Geometric Fidelity

This significantly high spatial resolution is one of specific features of QPS-SAR_2. Therefore, geometric performance has to be evaluated. By comparing QPS-SAR_2 images to geographic maps, geometric fidelity can be evaluated. Google map of aerial photos derived GCPs can be a good reference of the geometric performance evaluation, pixel size, pixel-to pixel distances.

Fig. 2 shows Google map of aerial photo of Fukuoka, Japan (33°36’47.13”N, 130°24’36.08”) and QPS-SAR_2 image which is acquired at 21:23 on 23 February 2021. Since Google map was created using advanced surveying techniques including aerial surveying, it was considered to have high geometric fidelity, and the instrumental fidelity of QPS-SAR_2 was measured with reference to this.

(a) Google map of aerial photo

(b) QPS-SAR_2

Fig. 2. Comparison of aerial photo and QPS-SAR_2 image.

The following two GCPs are selected for evaluation of pixel-to-pixel distance performance,

GCP1: 33°36’33.03”N, 130°23’24.88”E, Alt=4m

GCP2: 33°36’13.36”N, 130°22’50.28”E, Alt=1m

Yellow colored points (two end points of pixels are colored in yellow) are indicated the locations of GCPs in Fig. 3. Fig. 3 shows superimposed image between QPS-SAR_2 image and Google map. As the result, it is found that the distance between two GCPs is 5.41 km ± 2m. Therefore, it is concluded that geometric fidelity of QPS-SAR_2 is around 2m.

Fig. 3. Locations of GCPs and the distance between two GCPs (Fukuoka).

Same experiment is conducted with the following GCPs for Tokyo scene (Tokyo dome area) of QPS-SAR_2 image,

GCP3 : 35° 42’ 08.40” N, 139° 45’ 18.27” E 6m

GCP4 : 35° 04’ 29.71” N, 139° 44’ 12.59” E 2.6m

As shown in Fig. 4, white colored line shows the distance between two GCPs and indicates 2.11 km± 2m. Therefore, geometric fidelity of QPS-SAR_2 is around 2m.

On the other hand, an attempt is made for estimation of off-nadir angle and SAR radio wave irradiation direction with Google Earth which can change azimuth and elevation of look angle. Fig. 5 shows the resultant image of superposed Tokyo Dome image of QPS-SAR_2 image on Google Earth derived aerial photo. Because the Tokyo Dome area is almost flat so that there is no shadowing, layover, and foreshortening. Therefore, the two images are almost perfectly matched. Thus, it is found that estimation of off-nadir angle and radio wave irradiation direction can be done with Google Earth. Geometric fidelity is defined as pixel geolocation knowledge which can be determined by the geometric parameters of off-nadir angle of SAR antenna, satellite nadir location (satellite position determination accuracy), Earth curvature at the footprint of SAR antenna pattern. Using image rotation (azimuth and elevation angles) and translation functions of Google Earth, QPS-SAR_2 image and Google Earth image can be matched. This implies that the rotation angle and translation pixels are almost same as the predicted value from the pixel geolocation knowledge, which is determined by satellite position knowledge, off-nadir angle, compliant Earth spheroidal model of WGS84[3].

Fig. 4. Locations of GCPs and the distance between two GCPs (Tokyo Dome).

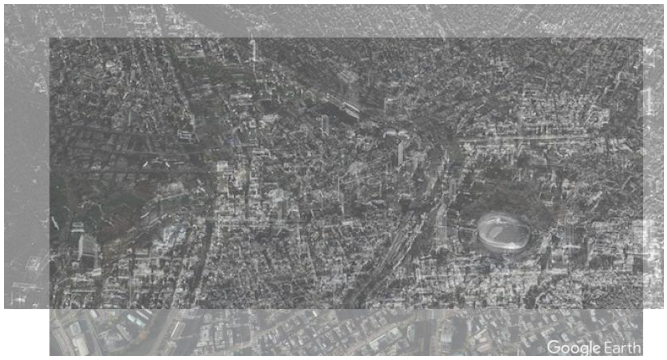

Fig. 5. Resultant image of superposed Tokyo Dome image of QPS-SAR_2 image on Google Earth derived aerial photo.

C. Saturated Pixel Ratio

On 23 March 2021 (Friday) of the QPS-SAR_2 data acquisition, the Sentinel-1 of SAR data is acquired Tokyo scene. Therefore, cross comparison between both images can be done. Fig. 6 shows the Tokyo scene of QPS-SAR_2 (a) and Sentinel-1/SAR images (b) and the superimposed QPS-SAR_2 image onto Sentinel-1/SAR image (c). On the other hand, Fig. 6 (d) to 6(h) show Sentinel-1/SAR VV polarization, VH polarization, QPS-SAR_2 HH polarization, simulated VH polarization and VV polarization. Although QPS-SAR_2 is essentially HH polarization, through the regression analysis[4], it was found that the VH and the VV polarization of QPS-SAR_2 can be derived from the following equations,

$$\text{VH-Pol} = 1.478\ \text{HH-Pol} + 15.24 \quad (1)$$

$$\text{VV-Pol} = 2.49\ \text{HH-Pol} + 21.32 \quad (2)$$

As shown in Fig. 6, the most visual difference between both is saturated pixels.

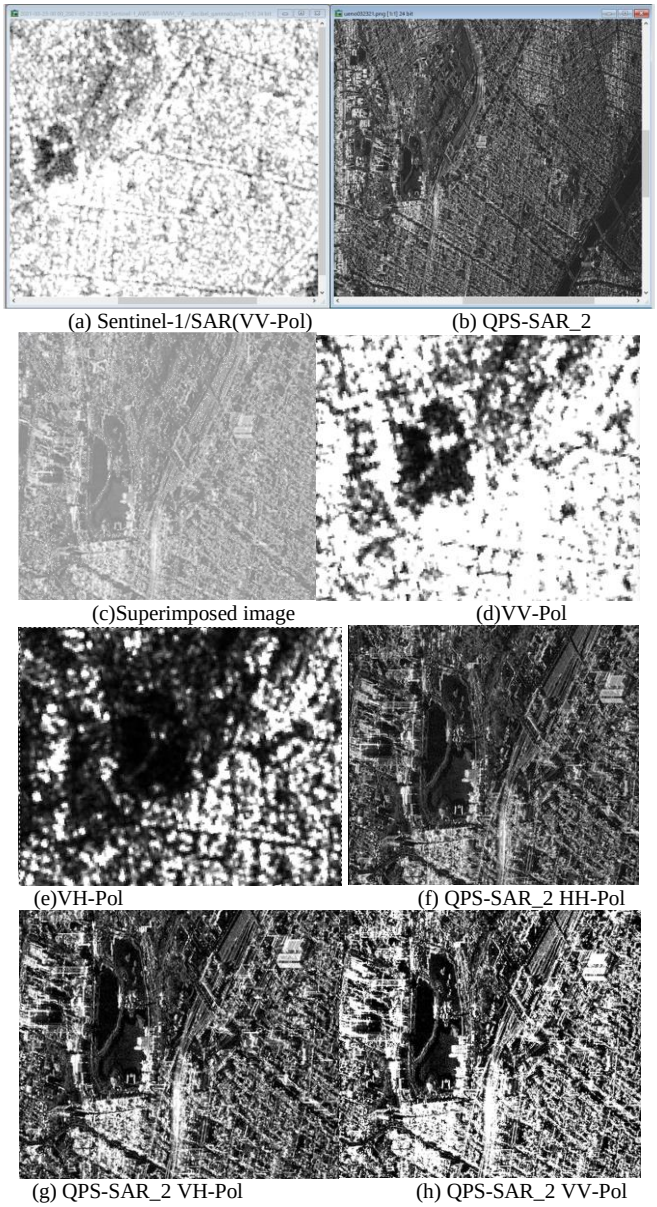

(a) Sentinel-1/SAR(VV-Pol) (b) QPS-SAR_2

(c)Superimposed image (d)VV-Pol

(e)VH-Pol (f) QPS-SAR_2 HH-Pol

(g) QPS-SAR_2 VH-Pol (h) QPS-SAR_2 VV-Pol

Fig. 6. Tokyo scene of QPS-SAR_2 and Sentinel-1/SAR images.

[3]The World Geodetic System 1984 (WGS 84) is a 3-dimensional coordinate reference frame for establishing latitude, longitude and heights for navigation,

[4]https://jp.mathworks.com/discovery/linear-regression.html

Saturated pixel ratios of the two different SAR imagery data are evaluated. As shown in Fig. 7, the saturated pixel ratio of Sentinel-1/SAR is 233.07/255=91.4 (%) while that of QPS-SAR_2 is 81.78/255=32.07 (%). Therefore, this QPS-SAR_2 image is much informative than that of Sentinel-1/SAR image in terms of non-saturated pixels. Since Sentinel-1/SAR has VV and VH polarizations, the saturation rate at VV becomes high. If the VV saturation rate is lowered and the dynamic range setting is matched to VV, the dynamic range of VH will be narrowed.

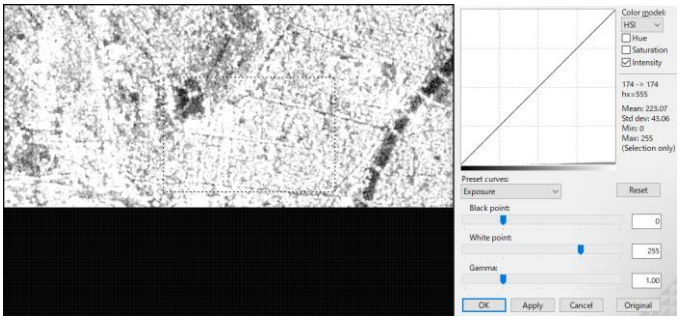

(a)Sentinel-1/SAR VV-Pol

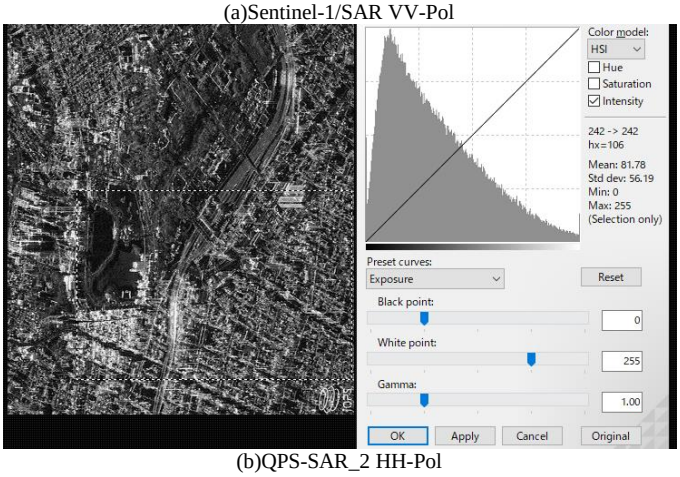

(b)QPS-SAR_2 HH-Pol

Fig. 7. Saturated pixel ratios of the two different SAR imagery data.

D. Frequency Component Analysis

Fig. 8 shows frequency components of QPS-SAR_2 and Sentinel-1/SAR imagery data of Tokyo Dome scene. As shown in Fig. 8, it is clear that the QPS-SAR_2 image shows much wider frequency components in comparison to that of the Sentinel-1/SAR image. The top left corner of the Fig. 8 shows zero frequency component, and the horizontal/vertical axis shows horizontal and vertical frequency components, respectively.

From the results of the aforementioned two experiments, following is found:

1) Sentinel-1/SAR concentrates on frequency components that are about 10 times lower than QPS-SAR_2.

2) It is reasonable because the spatial resolution of QPS-SAR_2 is 10 times smaller than that of Sentinel-1/SAR.

3) Saturation rate (average pixel value / 255): Sentinel-1/SAR VV-Pol is about 38.69 times higher than QPS-SAR_2 HH-Pol (Sentinel-1/SAR VV-Pol has many saturated pixels).

(a)QPS-SAR_2

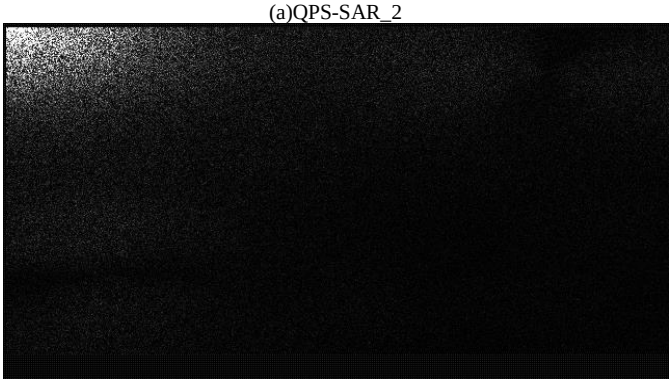

(b)Sentinel-1/SAR

Fig. 8. Frequency component comparison between QPS-SAR_2 and Sentinel-1/SAR.

E. Singal to Noise Ratio

Signal to noise ratio (S/N) depends on the intensity level, backscattering cross section.

Therefore, S/N is evaluated at low, middle and high levels of Fukuoka scene of QPS-SAR_2 image. As shown in Fig. 9, it is found that the low level of S/N=44.18/3.25=13.59, the middle level of S/N=55.52/6.72=8.26, and the high level of S/N=148.33/38.91=3.18. Noise component is mainly caused by speckle noise of which the footprint composed with multiple targets (Due to radio wave interference from multiple targets). In comparison among the low, the middle and the high levels of QPS-SAR_2 image, the number of pixels which composed with multiple targets for the low levels of image is small and that for the middle level of image is middle in between small and large as well as that for the high level is large.

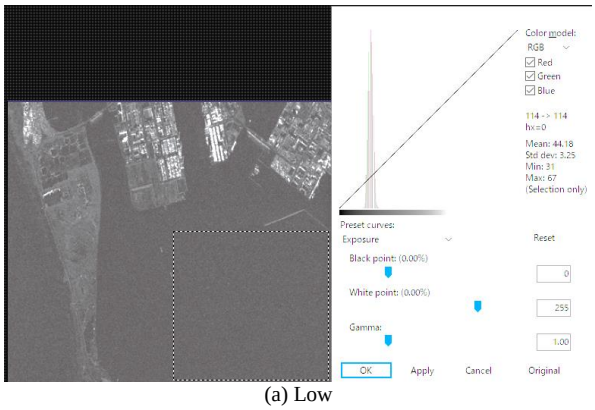

(a) Low

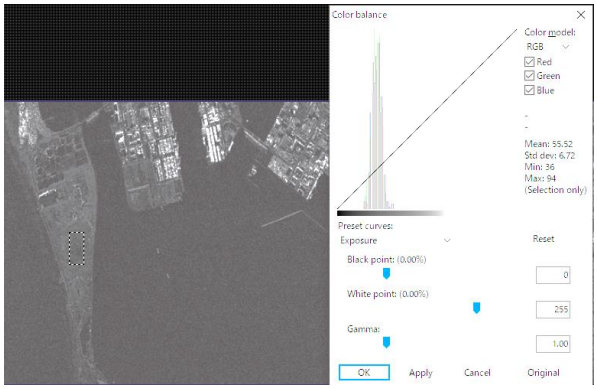

(b) Middle

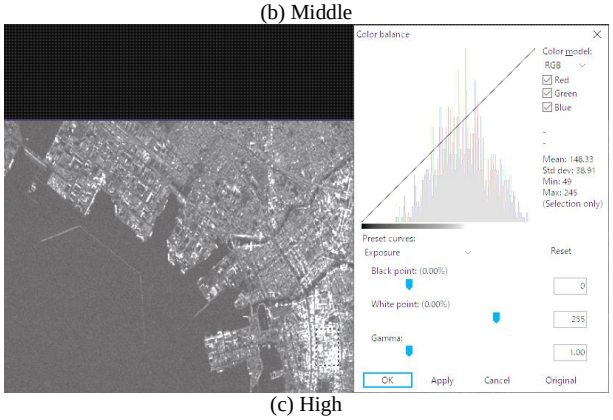

(c) High

Fig. 9. S/N evaluation for low, middle and high intensity levels with Fukuoka scene of QPS-SAR_2 image.

F. Speckle Noise Reduction

When observing a distributed target, speckle noise is generated by the fading phenomenon caused by the random presence of a large number of scatterers in the resolution cell, so this detection and reduction is necessary. The important thing of the speckle noise reduction is filter kernel size and filter function. In this paper, comparisons are made between 3 by 3 and 5 by 5 of kernel sizes for median filter, as well as between circle and Gauss filter functions. The circle and the Gauss filters are well known and widely used typical kernel spatial filter functions without edge preservation. On the other hand, the median filter with the kernel size of 3 and 5 are edge preserving filter. Frequency component is degraded depending on the kernel size and the kernel functions. Fig. 10 shows the resultant images of the comparisons. As the result, it is found that the best filter kernel size is 3 by 3 and the filter function of Gauss is much better than the circle filter function through visual comparison. From the point of view of spatial frequency component preservation, the median filter with 3 by 3 filter kernel shows the best performance, obviously.

(a)3 by 3 of median filter (b)5 by 5 of median filter

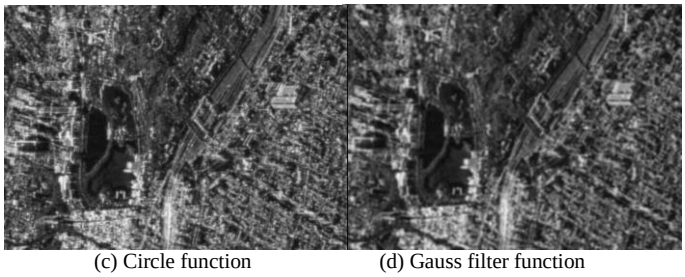

(c) Circle function (d) Gauss filter function

Fig. 10. Comparisons between 3 by 3 and 5 by 5 of kernel sizes for median filter, as well as between circle and Gauss filter functions.

V. Discussion

Although SAR image quality evaluation methods such as spatial resolution, signal to noise ratio, modulation transfer function, pixel geolocation accuracy (geometric fidelity), etc. are confirmed through the experiments, speckle noise reduction is not good enough. Multiple or single target in the footprint is the issue of the speckle noise reduction. Therefore, further thoughts considering the causes of the speckle noise are required for improvement of noise reduction performance.

VI. Conclusion

Method for image quality evaluation of satellite-based SAR data is proposed. Not only geometric fidelity but also S/N, Frequency component, saturated pixel ratio, speckle noise, optimum filter kernel size and its filter function are evaluated. Through experiments with Q-shu Pioneers of Space: QPS-SAR_2 imagery data, all these items are evaluated, and it is confirmed that the geometric and radiometric performances are good enough. Also, geometric fidelity of QPS-SAR_2 is compared to Sentinel-1/SAR of ESA provided data which is obtained on the same day of QPS-SAR_2 data acquisition.

In more detail, the S/N of QPS-SAR_2 was found to be 3.18 to 13.59 for the Fukuoka image and 1.96 to 5.10 for the Tokyo image. Also, it was found that the wind size suitable for speckle noise removal is 3x3, and Gauss is suitable for the filter function. Furthermore, Sentinel-1/SAR concentrates on frequency components that are about 10 times lower than QPS-SAR_2. Moreover, spatial resolution is about 10 times lower for Sentinel-1/SAR than for QPS-SAR_2. Meanwhile, saturation rate (average pixel value / 255): Sentinel-1/SAR is about 38.69 times higher than QPS-SAR_2 so that Sentinel-1/SAR may have more saturated pixels than QPS-SAR_2.

Future Research Works

In the future, we will evaluate layover, shadowing, fore shortening, and signal to ambiguity ratio, main lobe / first side lobe ratio, spatial resolution, radiometric resolution, etc. using QPS-SAR_2 images which observe corner reflectors and with ground test data.

Acknowledgment

The authors would like to thank Professor Dr. Hiroshi Okumura and Professor Dr. Osamu Fukuda for their technical discussions.

REFERENCES

[1] Kohei Arai, and N.Fujimoto, GCP acquisition using simulated SAR derived from DEM, Proc.of the ISPRS Symposium, 33-40, 1988.

[2] Kohei Arai, GCP Acquisition Using Simulated SAR and Evaluation of GCP Matching Accuracy with Texture Features, International Journal of Remote Sensing, Vol.12, No.11, pp.2389-2397, Oct.1991.

[3] H.Wakabayashi and Kohei Arai, Speckle noise removal of SAR images with Digital Elevation Model: DEM, Proc. of the 5th ISCOPS Symposium, 1993.

[4] H. Wakabayashi and Kohei Arai, A method of Speckle Noise Reduction for SAR Data, International Journal of Remote Sensing, Vol.17, No.10, pp.1837-1849, May 1995.

[5] Kohei Arai and Y.Terayama, SAR image classification based on Maximum Likelihood Decision rule with texture features taking into account a fitness to the probability density function, Final Report of JERS-1/ERS-1 System Verification Program, J2, vol.II, pp.2-415 to 424, Munich, Mar., 1995.

[6] H. Wakabayashi and Kohei Arai, A New Method for SAR Speckle Noise Reduction (Chi-Square Filter), Canadian Journal of Remote Sensing, Vol.22, No.2, pp.190-197, Jun.1995.

[7] H.Wakabayashi and Kohei Arai, A New Method for SAR Speckle Noise Reduction (Chi-Square Test Filter), Canadian journal of Remote Sensing, Vol.22, No.2, pp.190-197, June 1996.

[8] Kohei Arai Decomposition of SAR Polarization Signatures by Means of Eigen-Space Representation, Proc. of the Synthetic Aparture Radar Workshop '98, 1998

[9] N.Ebuchi, Kohei Arai, et.al., Evaluation of vector winds observed by NSCAT in the seas around Japan, Journal of Ocean Society of Japan, Vol.56, No.5, pp.495-505,(2000).

[10] Kohei Arai and Wang June, Polarimetric SAR image classification with maximum curvature of the trajectory in eigen space domain on the polarization signature, Abstracts of the 35th Congress of the Committee on Space Research of the ICSU, A3.1-0061-04, (2004)

[11] Kohei Arai and J.Wang, Polarimetric SAR image classification with maximum curvature of the trajectory in eigen space domain on the polarization signature, Advances in Space Research, 39, 1, 149-154, 2007.

[12] Kohei Arai, Polarimetric SAR image classification with high frequency component derived from wavelet multi resolution analysis: MRA, International Journal of Advanced Computer Science and Applications, 2, 9, 37-42, 2011.

[13] Kohei Arai Comparative study of polarimetric SAR classification methods including proposed method with maximum curvature of trajectory of backscattering cross section in ellipticity and orientation angle space, International Journal of Research and Reviews on Computer Science, 2, 4, 1005-1009, 2011.

[14] Kohei Arai, Wavelet Multi-Resolution Analysus and Its Application to Polarizatic SAR Classification, Proceeding of the SAI Computing Conference 2016,

[15] Kohei Arai, Sentinel 1A SAR Data Analysis for Disaster Mitigation in Kyushu, Kyushu Brunch of the Japanese Society on Remote Sensing, Special Lecture for Young Engineers on Remote Sensing, Nagasaki University, 2018.

[16] Kohei Arai, Hiroshi Okumura, Shogo Kajiki, Flood Damage Area Detection Method by Means of Coherency Derived from Interferometric SAR Analysis with Sentinel-1A SAR, International Journal of Advanced Computer Science and Applications IJACSA, 11, 7, 88-94, 2020.

[17] Kohei Arai, Ground Control Point Generation from Simulated SAR Image Derived from Digital Terrain Model and its Application to Texture Feature Extraction, International Journal of Advanced Computer Science and Applications, Vol. 12, No. 1, 89-94, 2021.

[18] Kohei Arai, Report on Vicarious Calibration and Image Quality Evaluation of LISA/LISAT, LAPAN Indonesia, May, 2018.

[19] Kohei Arai, Methods for Vicarious Calibration and Image Quality Evaluation of LISA/LISAT, LAPAN Indonesia, April, 2018.

[20] Kohei Arai, Polarimetric SAR image classification with high frequency component derived from wavelet multi resolution analysis: MRA, International Journal of Advanced Computer Science and Applications, 2, 9, 37-42, 2011.

[21] Kohei Arai, Takuto Konishi, Hearing aid method by equalizing frequency response of phoneme extracted from human voice, International Journal of Advanced Computer Science and Applications IJACSA, 8, 7, 88-93, 2017.

[22] Kohei Arai, T.Fukamachi, H.Okumura, S.Kawakami, H.Ohyama, Sensitivity analysis of Fourier Transformation Spectrometer: FTS against observation noise on retrievals of carbon dioxide and methane, International Journal of Advanced Computer Science and Applications, 3, 11, 58-64, 2012.

[23] Kohei Arai, Noise suppressing edge enhancement based on Genetic Algorithm taking into account complexity of target image measured with Fractal dimension, International Journal of Advanced Research in Artificial Intelligence, 2, 10, 7-13, 2013.

[24] Kohei Arai, Method for Aerosol Parameter Estimation Error Analysis-Consideration of Noises Included in the Measured Solar Direct and Diffuse Irradiance, International Journal of Advanced Research on Artificial Intelligence, 5, 11, 1-9, 2016.

[25] K.Tsuchiya, K.Maeda, Kohei Arai, H.Nakamura and C.Ishida, Method of noise reduction in passive remote sensing, Proc.of the International Symposium on Noise and Clutter Rejection, 1-8, 1984.

[26] H.WakabKasurishi and Kohei Arai, Speckle noise removal of SAR images with Digital Elevation Model: DEM, Proc. of the 5th ISCOPS Symposium, 1993.

[27] Kohei Arai, Hiroshi Okumura, Shogo Kajiki, Flood Damage Area Detection Method by Means of Coherency Derived from Interferometric SAR Analysis with Sentinel-1A SAR, International Journal of Advanced Computer Science and Applications IJACSA, 11, 7, 88-94, 2020.

[28] Kohei Arai, Ground Control Point Generation from Simulated SAR Image Derived from Digital Terrain Model and its Application to Texture Feature Extraction, International Journal of Advanced Computer Science and Applications, Vol. 12, No. 1, 89-94, 2021.

[29] Kohei Arai, Yushin Nakaoka, Osamu Fukuda1, Nobuhiko Yamaguchi1, Wen Liang Yeoh and Hiroshi Okumura, Method for Frequent High Resolution of Optical Sensor Image Acquisition Using Satellite-Based SAR Image for Disaster Mitigation, International Journal of Advanced Computer Science and Applications, 14, 3, 119-125, 2023.

AUTHOR'S PROFILE

Kohei Arai, He received BS, MS and PhD degrees in 1972, 1974 and 1982, respectively. He was with The Institute for Industrial Science and Technology of the University of Tokyo from April 1974 to December 1978 also was with National Space Development Agency of Japan from January 1979 to March 1990. During from 1985 to 1987, he was with Canada Centre for Remote Sensing as a Post-Doctoral Fellow of National Science and Engineering Research Council of Canada. He moved to Saga University as a Professor in Department of Information Science in April 1990. He is now an Emeritus Professor of Saga University since 2014. He was a council member for the Aeronautics and Space related to the Technology Committee of the Ministry of Science and Technology during from 1998 to 2000. He was a councilor of Saga University for 2002 and 2003. He also was an executive councilor for the Remote Sensing Society of Japan for 2003 to 2005. He is a Science Council of Japan Special Member since 2012. He is an Adjunct Professor of University of Arizona, USA since 1998 and is an Adjunct Professor of Nishi-Kyushu University as well as Kurume Institute of Technology/AI Application Laboratory since 2021. He was Vice Chairman of the Science Commission "A" of ICSU/COSPAR since 2008. He is now award committee member of ICSU/COSPAR. He wrote 78 books and published 695 journal papers as well as 560 conference papers. He received 77 of awards including ICSU/COSPAR Vikram Sarabhai Medal in 2016, and Science award of Ministry of Mister of Education of Japan in 2015. He is now Editor-in-Chief of IJACSA and IJISA. http://teagis.ip.is.saga-u.ac.jp/index.html